

## Coupled Oxidation vs Heme Oxygenation: Insights from Axial Ligand Mutants of Mitochondrial Cytochrome $b_5$

Ludivina Avila,<sup>†</sup> Hong-wei Huang,<sup>‡</sup> Christopher O. Damaso,<sup>†</sup> Shen Lu,<sup>‡</sup>  
Pierre Moëgne-Loccoz,<sup>‡</sup> and Mario Rivera<sup>\*†</sup>

Contribution from the Department of Chemistry, Oklahoma State University,  
Stillwater, Oklahoma 74078-3071, and Department of Biochemistry and Molecular Biology,  
OGI School of Science and Engineering at OHSU, Beaverton, Oregon 97006-8921

Received November 12, 2002; E-mail: rivera@okstate.edu

**Abstract:** Mutation of His-39, one of the axial ligands in rat outer mitochondrial membrane cytochrome  $b_5$  (OM cyt  $b_5$ ), to Val produces a mutant (H39V) capable of carrying out the oxidation of heme to biliverdin when incubated with hydrazine and  $O_2$ . The reaction proceeds via the formation of an oxyferrous complex ( $Fe^{II}-O_2$ ) that is reduced by hydrazine to a ferric hydroperoxide ( $Fe^{III}-OOH$ ) species. The latter adds a hydroxyl group to the porphyrin to form *meso*-hydroxyheme. The observation that catalase does not inhibit the oxidation of the heme in the H39V mutant is consistent with the formation of a coordinated hydroperoxide ( $Fe^{III}-OOH$ ), which in heme oxygenase is the precursor of *meso*-hydroxyheme. By comparison, mutation of His-63, the other axial ligand in OM cyt  $b_5$ , to Val results in a mutant (H63V) capable of oxidizing heme to verdoheme in the absence of catalase. However, the oxidation of heme by H63V is completely inhibited by catalase. Furthermore, whereas the incubation of  $Fe^{III}$ -H63V with  $H_2O_2$  leads to the nonspecific degradation of heme, the incubation of  $Fe^{II}$ -H63V with  $H_2O_2$  results in the formation of *meso*-hydroxyheme, which upon exposure to  $O_2$  is rapidly converted to verdoheme. These findings revealed that although *meso*-hydroxyheme is formed during the degradation of heme by the enzyme heme oxygenase or by the process of coupled oxidation of model hemes and hemoproteins not involved in heme catabolism, the corresponding mechanisms by which *meso*-hydroxyheme is generated are different. In the coupled oxidation process  $O_2$  is reduced to noncoordinated  $H_2O_2$ , which reacts with  $Fe^{II}$ -heme to form *meso*-hydroxyheme. In the heme oxygenation reaction a coordinated  $O_2$  molecule ( $Fe^{II}-O_2$ ) is reduced to a coordinated peroxide molecule ( $Fe^{III}-OOH$ ), which oxidizes heme to *meso*-hydroxyheme.

### Introduction

Heme serves as the prosthetic group in numerous hemoproteins that are essential to life. Heme-containing proteins are involved in a remarkably versatile array of important biological functions, including oxygen binding (hemoglobin and myoglobin), oxygen metabolism (monooxygenases and peroxidases), electron-transfer reactions (cytochromes), and signal transduction (guanylate cyclase, nitric oxide synthase). Cellular heme levels appear to be tightly controlled by a highly tuned interplay between heme biosynthesis and heme catabolism.<sup>1</sup> In mammals the only physiological path of heme catabolism starts when the enzyme heme oxygenase (HO) binds heme and in a series of electron- and dioxygen-dependent steps oxidizes heme to biliverdin, carbon monoxide (CO), and iron.<sup>2,3</sup> On the basis of spectroscopic<sup>4–6</sup> and X-ray crystallographic<sup>7,8</sup> studies it has been

established that the heme in the heme–HO complex is coordinated by a proximal His residue and by a distal  $H_2O$  or  $OH^-$  ligand. The X-ray structures revealed that there are no polar side chains (i.e., histidine) in close proximity to form a hydrogen bond to the coordinated water, as is the case for myoglobin.<sup>9</sup>

The catalytic cycle of HO (Scheme 1) parallels that of cytochrome P450 in that the ferric enzyme is reduced to its ferrous state, followed by the formation of an oxyferrous complex ( $Fe^{II}-O_2$ ). The latter accepts a second electron from NADPH cytochrome P450 reductase, and is thereby transformed into an activated hydroperoxy ( $Fe^{III}-OOH$ ) oxidizing species.<sup>10</sup> This oxidizing species adds a hydroxyl group to the  $\alpha$ -*meso* carbon to give  $\alpha$ -*meso*-hydroxyheme (Scheme 1). The  $\alpha$ -*meso*-hydroxyheme undergoes a subsequent  $O_2$ -dependent elimination of the hydroxylated  $\alpha$ -*meso* carbon as CO, with the concomitant

\* Address correspondence to this author.

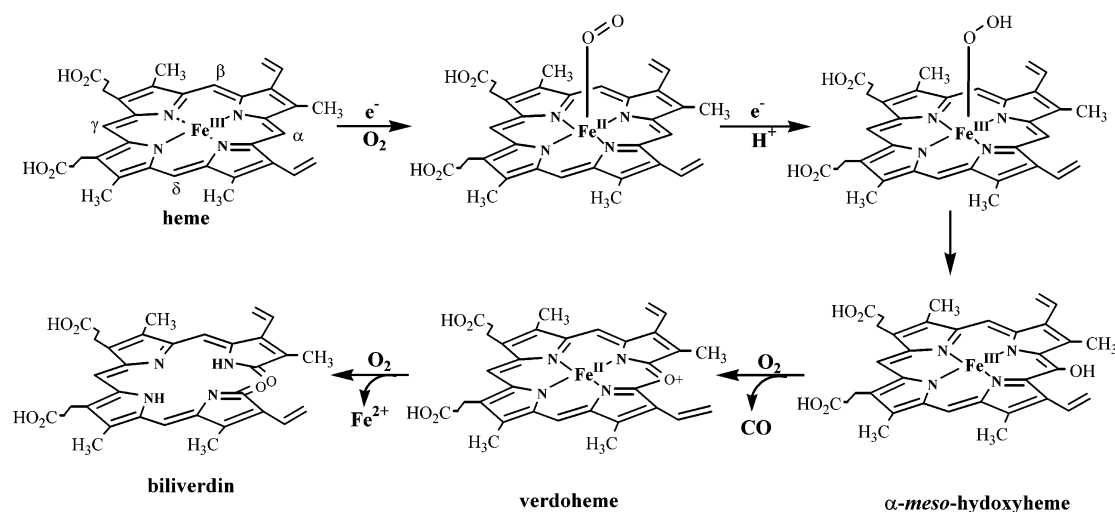
<sup>†</sup> Oklahoma State University.

<sup>‡</sup> OGI School of Science and Engineering at OHSU.

- (1) Ponka, P. *Am. J. Med. Sci.* **1999**, *318*, 241–256.
- (2) Maines, M. D. *Annu. Rev. Pharmacol. Toxicol.* **1997**, *37*, 517–554.
- (3) Ortiz de Montellano, P. R. *Acc. Chem. Res.* **1998**, *31*, 543–549.
- (4) Sun, J.; Wilks, A.; Ortiz de Montellano, P. R.; Loefer, T. M. *Biochemistry* **1993**, *32*, 14151–14157.
- (5) Sun, J.; Loefer, T.; Wilks, A.; Ortiz de Montellano, P. R. *Biochemistry* **1994**, *33*, 13734–13740.

- (6) Ito-Maki, M.; Kazunobu, I.; Matera, K. M.; Sato, M.; Ikeda-Saito, M.; Yoshida, T. *Arch. Biochem. Biophys.* **1995**, *317*, 253–258.
- (7) Schuller, D. J.; Wilks, A.; Ortiz de Montellano, P. R.; Poulos, T. L. *Nat. Struct. Biol.* **1999**, *6*, 860–867.
- (8) Schuller, D. J.; Zhu, W.; Stojiljkovic, I.; Wilks, A.; Poulos, T. L. *Biochemistry* **2001**, *40*, 11552–11558.
- (9) Springer, B. A.; Sligar, S. G.; Olson, J. S.; Phillips Jr., G., N. *Chem. Rev.* **1994**, *94*, 699–714.
- (10) Yoshida, T.; Noguchi, M.; Kikuchi, G. *J. Biol. Chem.* **1980**, *255*, 4418–4420.

Scheme 1



formation of verdoheme. Verdoheme is then oxidized to Fe<sup>III</sup>-biliverdin in a reaction that requires both O<sub>2</sub> and reducing equivalents.<sup>11,12</sup>

Mammalian heme oxygenases are membrane-bound enzymes and therefore are relatively difficult to overexpress and purify. Important progress toward the understanding of HO activity has been facilitated by the bacterial expression and characterization of a soluble fragment of mammalian HO.<sup>13,14</sup> Prior to this breakthrough, the coupled oxidation of myoglobin was used as a model to gain insight into the mechanism of heme oxygenation.<sup>15–17</sup> Coupled oxidation is a process in which a hemoprotein, or an iron porphyrin, is incubated with O<sub>2</sub> and a reducing agent such as ascorbic acid or hydrazine to oxidize the heme active site or the iron porphyrin to verdoheme and biliverdin.<sup>18</sup> The coupled oxidation reaction proceeds via the formation of the same intermediates observed during the oxidation of heme by HO, namely, *meso*-hydroxyheme and verdoheme (see Scheme 1).<sup>19</sup> It has been recognized that although the coupled oxidation reaction closely resembles the heme oxygenation process carried out by HO, the mechanistic details for both processes may not be identical. An important difference is that whereas the oxidation of heme by HO produces exclusively α-biliverdin, the coupled oxidation of protoheme IX in pyridine solution produces all four isomers of biliverdin, the coupled oxidation of heme in hemoglobin results in the formation of α- and β-biliverdin,<sup>20</sup> and the coupled oxidation of the heme in myoglobin produces exclusively α-*meso*-biliverdin,<sup>20</sup> although there is at least one report indicating that the coupled oxidation of myoglobin results in the formation of all four biliverdin isomers and that the ratio of isomers varies from experiment to experiment.<sup>21</sup> More recent studies on the coupled oxidation of

the heme in myoglobin have focused on the issue of regioselectivity; thus, the coupled oxidation of sperm whale myoglobin mutants in which the distal histidine (His-64) was relocated within the distal cavity was recently studied with the aim of understanding the factors that influence the regioselectivity of heme oxygenation.<sup>22</sup> It was observed that relocation of the distal histidine through F43H/H64L produced 40%, 16%, and 44% α-, β-, and γ-biliverdin, respectively, whereas F43W/H64L produced 33% α-biliverdin, 61% γ-biliverdin, and approximately 3% each of the β- and δ-isomers. These observations led the authors to the conclusion that the polarity of the active site, as well as hydrogen bonding of the O<sub>2</sub> molecule within the distal cavity of myoglobin, influences the regioselectivity of heme oxygenation.<sup>22</sup> It is noteworthy, however, that the coupled oxidation of myoglobin has been found to be inhibited by the hydrogen peroxide scavenger catalase, therefore suggesting that noncoordinated H<sub>2</sub>O<sub>2</sub> is the oxidant that brings about the coupled oxidation of the heme in myoglobin.<sup>23</sup> This finding strongly suggests that the coupled oxidation of myoglobin proceeds via a mechanism that is distinct from that followed by heme oxygenase (shown in Scheme 1), even if the same stable intermediates (*meso*-hydroxyheme and verdoheme) that are isolated during heme oxygenation are also isolated during the coupled oxidation of myoglobin. Consequently, the mechanism of coupled oxidation must be better understood before firm conclusions regarding heme oxygenation can be drawn from studying the coupled oxidation of myoglobin.

In recent years it has been shown that certain heme-containing electron-transfer proteins can be made to acquire coupled oxidation activity simply by mutating one of the axial ligands for a weakly coordinating or noncoordinating residue;<sup>24–27</sup> thus, a mutant of outer mitochondrial membrane (OM) cytochrome *b*<sub>5</sub> (cyt *b*<sub>5</sub>) in which one of the axial histidine ligands (His-63) has been replaced by Met, is capable of oxidizing heme to verdoheme when incubated with O<sub>2</sub> and hydrazine.<sup>24,25</sup> A similar

- (11) Yoshida, T.; Kikuchi, G. *J. Biol. Chem.* **1978**, *253*, 4230–4236.
- (12) Yoshida, T.; Noguchi, M.; Kikuchi, G. *J. Biochem.* **1980**, *88*, 557–563.
- (13) Ishikawa, K.; Sato, M.; Ito, M.; Yoshida, T. *Biochem. Biophys. Res. Commun.* **1992**, *182*, 981–986.
- (14) Wilks, A.; Ortiz de Montellano, P. R. *J. Biol. Chem.* **1993**, *268*, 22357–22362.
- (15) Brown, S. B. *Biochem. J.* **1976**, *159*, 23–27.
- (16) Brown, S. B.; King, R. F. G. *Biochem. J.* **1978**, *170*, 297–311.
- (17) Brown, S. B.; King, R. F. G. *J. Biochem. Soc. Trans.* **1976**, *4*, 197–201.
- (18) Lemberg, R. *Rev. Pure Appl. Chem.* **1956**, *6*, 1–23.
- (19) Sano, S.; Sano, T.; Morishima, I.; Shiro, Y.; Maeda, Y. *Proc. Natl. Acad. Sci. U.S.A.* **1986**, *83*, 531–535.
- (20) O'Carra, P.; Collieran, E. *FEBS Lett.* **1969**, *5*, 295–298.
- (21) Sakamoto, H.; Omata, Y.; Palmer, G.; Noguchi, M. *J. Biol. Chem.* **1999**, *274*, 18196–18200.

- (22) Murakami, T.; Morishima, I.; Toshitaka, M.; Ozaki, S.-i.; Hara, I.; Yang, H.-J.; Watanabe, Y. *J. Am. Chem. Soc.* **1999**, *121*, 2007–2011.
- (23) Sigman, J. A.; Wang, X.; Lu, Y. *J. Am. Chem. Soc.* **2001**, *123*, 6945–6946.
- (24) Rodriguez, J. C.; Rivera, M. *Biochemistry* **1998**, *37*, 13082–13090.
- (25) Rodriguez, J. C.; Desilva, T.; Rivera, M. *Chem. Lett.* **1998**, 353–354.
- (26) Avila, L.; Huang, H.-w.; Rodriguez, J. C.; Moënne-Loccoz, P.; Rivera, M. *J. Am. Chem. Soc.* **2000**, *122*, 7618–7619.
- (27) Rice, J. K.; Fearnley, I. M.; Barker, P. D. *Biochemistry* **1999**, *38*, 16847–16856.

finding was made when the His axial ligand of cytochrome  $b_{562}$  was replaced by methionine.<sup>27</sup> It was suggested that the coupled oxidation of the heme in the OM cytochrome  $b_5$  and cytochrome  $b_{562}$  mutants stops at verdoheme as a consequence of the formation of a hexacoordinate verdoheme complex, which is axially coordinated by His-39 and Met-63 in OM cytochrome  $b_5$ ,<sup>24</sup> and by Met-7 and Met-102 in cytochrome  $b_{562}$ .<sup>27</sup> Two additional axial ligand mutants of OM cytochrome  $b_5$ , H63V and H39V, have been prepared with the aim of eliminating the coordination of verdoheme by a putative sixth ligand, thus preventing the possibility that the coupled oxidation process is arrested at the verdoheme stage due to the formation of a hexacoordinate verdoheme complex.<sup>26</sup> These investigations demonstrated that the coupled oxidation of the heme in the H63V mutant is still arrested at the verdoheme stage, while in contrast the coupled oxidation of the H39V mutant results in the initial accumulation of an oxyheme complex that is gradually oxidized to produce biliverdin.<sup>26</sup> These observations suggest that the coupled oxidation of the H39V mutant might occur via a mechanism different from that followed by H63V and that exploring the mechanism by which the two axial ligand mutants oxidize their hemes might yield some insight into the potential mechanistic differences between heme oxygenation and coupled oxidation. As will be shown below, we find that the coupled oxidation of the heme in H63V is brought about by noncoordinated hydrogen peroxide; thus, the function of the sacrificial electron donor (hydrazine) is not limited to the reduction of the ferric protein but also includes the reduction of noncoordinated  $O_2$  to noncoordinated  $H_2O_2$ . Furthermore, the coupled oxidation process is carried out by a reaction between the ferrous protein and hydrogen peroxide that results in the formation of *meso*-hydroxyheme. In contrast, the coupled oxidation of the H39V mutant is not inhibited by catalase and is carried out via the reduction of coordinated  $O_2$  ( $Fe^{II}-O_2$ ), which results in the formation of coordinated  $H_2O_2$  ( $Fe^{III}-OOH$ ), the oxidizing species known to be involved in the heme oxygenation process carried out by HO.

## Experimental Procedures

**Site-Directed Mutagenesis and Protein Expression.** The recombinant plasmid MRL1<sup>28</sup> and the transformer site-directed mutagenesis kit (Clontech) were used to construct the rat OM cyt  $b_5$  mutants, following a protocol outlined previously.<sup>24</sup> The sequences corresponding to the mutagenic primers designed to introduce the H63V and H39V mutations, and that corresponding to the selection primer (*Aj/III* to *Bg/III*) are 5'-CCGAATCTTTCGAAGATGTTGGCGTGTCTCCGGATGCGCG-3', 5'-CCGAATCTTTCGAAGATGTTGGCGTGTCTCCGGATGCGCG-3', and 5'-GGGATAACGCAGGAAAGAAGATCTGAGCAAAAG-GCC-3', respectively. The italic codons represent mismatches introduced to generate the mutations. Protein expression and purification of the variants was carried out following a procedure similar to that described by Rodriguez et al.<sup>24</sup> In brief, 1.0 L of LB medium was inoculated with 5 mL of an *E. coli* BL21(DE3) culture grown overnight. When the OD<sub>600</sub> reached a value of 0.80–1.0, biosynthesis of the polypeptide was induced by adding IPTG (isopropyl  $\beta$ -thiogalactoside) to a final concentration of 1.0 mM, followed by the addition of 17 mg of aminolevulinic acid and 100 mg of  $FeSO_4 \cdot 7H_2O/L$  of cell culture. Cells were harvested by centrifugation 2.5 h after induction of protein synthesis, cell debris was separated by ultracentrifugation, and the supernatant was made 3 mM in  $K_3Fe(CN)_6$  and 1 mM in imidazole,

previous to dialysis at 4.0 °C against ion-exchange buffer (10 mM EDTA, 50 mM Tris, and 1.0 mM imidazole, pH 7.8). The desalted solution was loaded onto an anion-exchange resin (DE52, Whatman) previously equilibrated with ion-exchange buffer and eluted with a linear salt gradient (0.0–0.50 M NaCl) containing 1.0 mM imidazole. The pooled fractions were then reconstituted with hemin. Hemin solutions were prepared by dissolving 10 mg of hemin (Porphyrin Products, Utah) in 300  $\mu$ L of  $CHCl_3$  and 100  $\mu$ L of pyridine; the  $CHCl_3$  and pyridine were evaporated under a stream of argon, hemin was redissolved in 0.1 M NaOH, and the pH of the resultant solutions was adjusted to 7.5 with 0.1 M HCl. The protein was then dialyzed against gel filtration buffer (100 mM NaCl, 20 mM Tris, and 1.0 mM EDTA, pH 7.4), concentrated by ultrafiltration, and further purified by size-exclusion chromatography.

**Electronic Absorption and EPR Spectroscopy.** Experiments performed under inert atmosphere were typically conducted at 25 °C in a modified quartz cuvette connected to a Schlenk line. A solution of the appropriate ferric protein ( $\sim 10 \mu$ M) was degassed by bubbling Ar for at least 1 h through a polyethylene capillary tube (0.8 mm i.d.) inserted through a small port in the anaerobic cell. The capillary tube was then removed, the port was capped with a rubber septum, and the cell was maintained under slight positive pressure with the aid of the Schlenk line. The anaerobic ferric protein was then reduced with a solution of sodium dithionite, which was added with a gastight syringe through the rubber septum. Addition of other reagents, such as anaerobic solutions of hydrogen peroxide, was also carried out through the rubber septum with the aid of a gastight syringe. Rates of autoxidation of the oxyheme complexes were measured as follows: Anaerobic solutions of the appropriate ferric protein, thermostated at 17 °C, were reduced with sodium dithionite as described above. The resultant anaerobic solutions of ferrous protein were bubbled with air under constant stirring to form the corresponding oxyferrous complex, a reaction that is complete within 15 s. Electronic absorption spectra were subsequently collected with a UV-vis S2000 spectrophotometer (Ocean Optics, Dunedin, FL) at appropriate intervals to monitor the autoxidation of the oxyferrous complex. The corresponding rate constants were obtained by fitting the time-dependent decay of the peak at 577 nm to a single-exponential function, as reported previously.<sup>29</sup> Coupled oxidation reactions were conducted in the cell described above with solutions containing the appropriate cytochrome  $b_5$  mutant ( $\sim 10 \mu$ M) in 4.5 mL of 50 mM phosphate buffer, pH 8.5, at 25 °C. The coupled oxidation reaction was initiated by the addition of hydrazine to a final concentration of 0.5 mM; the solution was bubbled with  $O_2$ , and the progress of the reaction was monitored by electronic absorption spectroscopy at regular intervals. When appropriate, catalase was added to a final concentration of  $\sim 0.4 \mu$ M.

The concentration of hydrogen peroxide formed upon bubbling  $O_2$  through aqueous solutions containing hydrazine was determined, in accord with previously reported analytical methodology,<sup>30–32</sup> via the spectrophotometric determination of the triiodide ion ( $I_3^-$ ). The latter is formed when  $H_2O_2$  is added to a concentrated solution of  $I^-$ , a reaction that is catalyzed by ammonium molybdate. In short, a solution (15 mL) containing 0.50 mM hydrazine in phosphate buffer (pH 8.5) was bubbled with  $O_2$ , with constant stirring. Samples (3.0 mL) were drawn approximately every 1 h; each sample was treated with 1 M  $H_2SO_4$  to adjust the pH to 2.8 and then transferred to a cuvette, followed by the addition of 0.50 mL of KI (0.80 M) and 50  $\mu$ L of ammonium molybdate (0.5% weight by volume), under constant stirring. The electronic absorption spectrum was obtained 3 min after the addition of ammonium molybdate, and the concentration of  $I_3^-$  was determined

(29) Brantley, R. E.; Smerdon, S. J.; Wilkinson, A. J.; W., S. E.; Olson, J. S. *J. Biol. Chem.* **1993**, *268*, 6995–7010.

(30) Ovenston, T. C. J.; Rees, W. T. *Analyst* **1950**, *75*, 204–208.

(31) Patrick, W. A.; Wagner, H. B. *Anal. Chem.* **1949**, *21*, 1279–1280.

(32) Klassen, N. V.; Marchington, D.; E., M. H. C. *Anal. Chem.* **1994**, *66*, 2921–2925.

(28) Rivera, M.; Barillas-Mury, C.; Christensen, K. A.; Little, J. W.; Wells, M. A.; Walker, F. A. *Biochemistry* **1992**, *31*, 12233–12240.

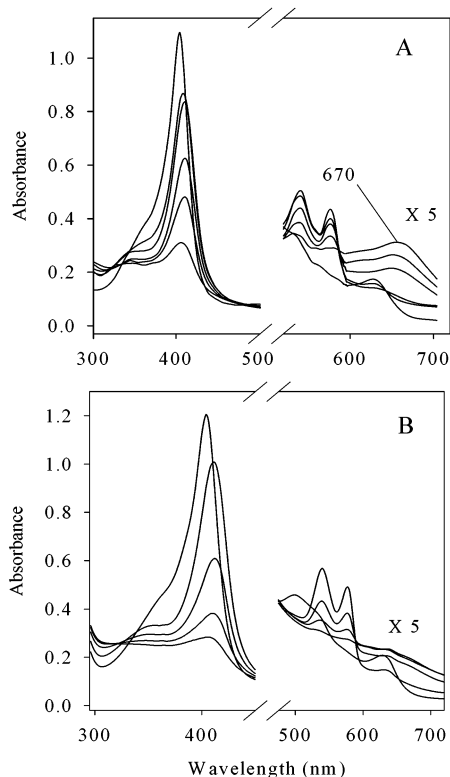


**Figure 1.** Electronic absorption spectra obtained during incubation of the H39V mutant with hydrazine and  $O_2$  in the presence (A) and in the absence (B) of catalase. Spectra were acquired every 20 min for a period of 2 h.

from the absorption at 351 nm ( $\epsilon_{351} = 25700 \text{ L}/(\text{mol cm}^{-1})$ ).<sup>33</sup> The blank consisted of 3.0 mL of a freshly prepared solution of hydrazine (0.50 mM) in phosphate buffer (pH 9.0), which was treated in a manner identical to that described above for the hydrazine solutions bubbled with  $O_2$ . The electronic absorption spectra obtained from the blank and from hydrazine solutions bubbled with  $O_2$  for 1 and 2.5 h are shown in the Supporting Information, Figure S1. EPR spectra were obtained on a Bruker E500 X-band EPR spectrometer equipped with a superX microwave bridge, a superhigh Q cavity, and a nitrogen flow cryostat.

## Results and Discussion

**Catalase Does Not Inhibit the Coupled Oxidation of the H39V Mutant of OM Cyt  $b_5$ .** It has been recently reported that the coupled oxidation of myoglobin is inhibited by the presence of catalase,<sup>23</sup> which suggests that the oxidant that hydroxylates the heme in myoglobin is noncoordinated  $H_2O_2$ ; the latter is likely to originate from the reduction of noncoordinated  $O_2$  by hydrazine.<sup>34</sup> It is therefore of interest to elucidate whether catalase has an inhibitory effect on the coupled oxidation of cytochrome  $b_5$  axial ligand mutants. When  $Fe^{III}$ -H39V is incubated with  $O_2$  and hydrazine, the following observations are made independent of whether catalase is present (Figure 1A) or absent (Figure 1B): During the initial stages of the reaction the oxyheme complex ( $Fe^{II}-O_2$ -H39V) is formed. This species reaches its maximum concentration within the first 15–20 min of reaction, as is evident by the fact that the bands at 540 and 577 nm (Figure 1), which are diagnostic of  $Fe^{II}-O_2$ -H39V, reach their maximum intensity in approximately 20 min. Thereafter, the intensity of these bands decreases with

the simultaneous appearance and growth of a broad band centered at 670 nm, suggesting that the product of the coupled oxidation of the heme-H39V complex is  $Fe^{III}$ -biliverdin. The nature of this product was investigated by extracting it into chloroform after unreacted heme had been removed by extraction with ethyl ether under acidic conditions. The electronic absorption spectrum of the product of the coupled oxidation reaction dissolved in chloroform is identical to the spectrum obtained from authentic biliverdin, thus corroborating that the latter is formed whether catalase is present or absent. It is also interesting to note that the yield of biliverdin is higher when the coupled oxidation is carried out in the presence of catalase, as can be seen from the relative intensity of the 670 nm bands in Figure 1A (with catalase) and 1B (without catalase). The higher yield of biliverdin is likely to originate from the protective role that catalase exerts by scavenging noncoordinated  $H_2O_2$ . In fact, if hydrogen peroxide is mixed with  $Fe^{III}$ -H39V, or with the oxyheme complex of H39V, the Soret band decreases in intensity, but neither verdoheme nor biliverdin is formed at detectable levels.

The fact that catalase does not inhibit the coupled oxidation of the heme-H39V complex, together with the observation that the oxyheme complex of H39V accumulates in the initial stages of the reaction, suggests that the coupled oxidation of the heme-H39V complex is brought about by a ferric hydroperoxo species ( $Fe^{III}-OOH$ ) formed by the reduction of coordinated  $O_2$  ( $Fe^{II}-O_2$ ). Additional evidence suggesting that the heme-H39V complex is oxidized by a coordinated hydroperoxide was obtained by reacting the oxyferrous complex of H39V with hydrazine in the presence of catalase. To this end,  $Fe^{III}$ -H39V was reduced with 1 equiv of sodium dithionite under anaerobic conditions. The anaerobic solution containing  $Fe^{II}$ -H39V was bubbled with air, which resulted in the immediate formation of the  $Fe^{II}-O_2$ -H39V complex, as is evident from the characteristic bands at 540 and 577 nm in the electronic absorption spectrum shown in Figure 2. If the solution containing  $Fe^{II}-O_2$ -H39V is allowed to stand in air, the oxyheme complex is autoxidized to  $Fe^{III}$ -H39V with a half-life of approximately 1 h (Figure 2A). It is apparent that the autoxidation of the  $Fe^{II}-O_2$ -H39V complex cleanly restores  $Fe^{III}$ -H39V, without significantly decreasing the intensity of the Soret band, thus indicating that the process of autoxidation does not cause heme destruction. On the other hand, if catalase and hydrazine are added immediately after the oxyferrous complex has been formed, the latter is transformed into biliverdin, as is apparent from the decrease in intensity of the bands located at 540 and 577 nm and the concomitant emergence and growth of a broad band at 670 nm (Figure 2B). The presence of catalase ensures that noncoordinated hydrogen peroxide is scavenged; hence, the oxidation of the oxyferrous complex to biliverdin upon addition of the sacrificial electron donor strongly suggests that the reaction proceeds by the reduction of coordinated dioxygen ( $Fe^{II}-O_2$ ) to coordinated hydroperoxide ( $Fe^{III}-OOH$ ), which presumably attacks the heme to form *meso*-hydroxyheme. The latter, in turn, is converted to verdoheme and then biliverdin in the presence of hydrazine.

**Catalase Inhibits the Coupled Oxidation of the H63V Mutant of OM Cytochrome  $b_5$ .** When  $Fe^{III}$ -H63V is incubated with  $O_2$  and hydrazine, a gradual decrease in the intensity of the Soret band is accompanied by the appearance and growth

(33) Bichsel, Y.; von Gunten, U. *Anal. Chem.* **1999**, *71*, 34–38.

(34) Audieth, L. F.; Ogg, B. A. *The Chemistry of Hydrazine*; Wiley: New York, 1951.

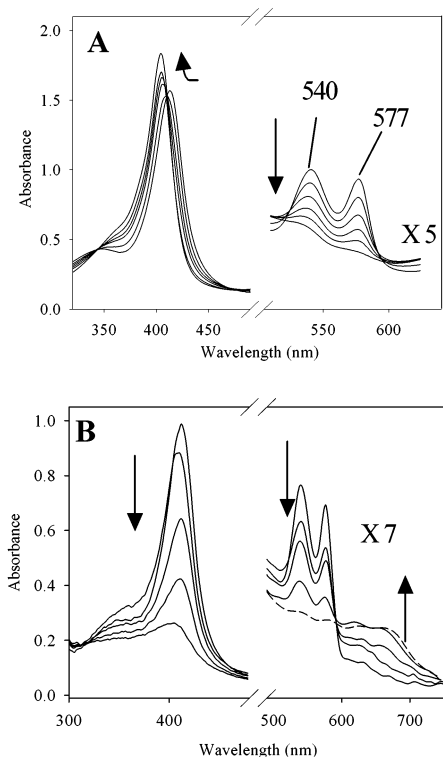


**Figure 2.** (A) Electronic absorption spectra obtained during the autoxidation of the Fe<sup>II</sup>-O<sub>2</sub>-H39V complex prepared by the addition of sodium dithionite to an anaerobic solution of Fe<sup>III</sup>-H39V, followed by exposure to air. (B) Electronic absorption spectra obtained upon addition of hydrazine and catalase to a solution containing Fe<sup>II</sup>-O<sub>2</sub>-H39V.

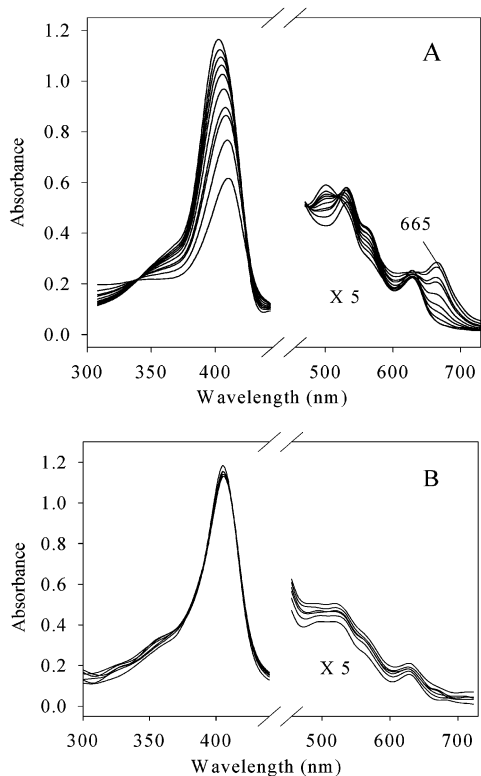


**Figure 3.** Electronic absorption spectra obtained during the coupled oxidation of the H63V mutant in the absence (A) and in the presence (B) of catalase. Spectra were acquired at 10 min intervals for 1.5 h.

of a band centered at 665 nm (Figure 3A). It has previously been demonstrated that the emergence and growth of a band at

665 nm during the coupled oxidation process is diagnostic of the formation of verdoheme.<sup>24,26</sup> This was corroborated by the electronic absorption spectrum of the reaction product extracted into a chloroform-pyridine solution, which is identical to that previously reported for authentic verdohemochrome.<sup>35-37</sup> In stark contrast, when Fe<sup>III</sup>-H63V is incubated with O<sub>2</sub> and hydrazine in the presence of catalase, the only spectral change that is observed corresponds to a slight decrease in the intensity of the Soret band (Figure 3B). It is therefore apparent that the presence of catalase inhibits the coupled oxidation of the heme in H63V by scavenging noncoordinated H<sub>2</sub>O<sub>2</sub>, which is presumably generated in the reaction mixture via the reduction of noncoordinated O<sub>2</sub> by hydrazine. In this context it is important to note that hydrogen peroxide is formed upon exposure of aqueous solutions of hydrazine to air or to an atmosphere of dioxygen.<sup>34,38</sup> The concentration of accumulated H<sub>2</sub>O<sub>2</sub> in these solutions is thought to depend on a balance between two reactions, one of formation and the other of decomposition.<sup>38</sup> Thus, hydrazine reduces O<sub>2</sub> to H<sub>2</sub>O<sub>2</sub>, and the latter oxidizes hydrazine to HN<sub>3</sub> and NH<sub>3</sub>.<sup>34</sup> To investigate whether significant concentrations of H<sub>2</sub>O<sub>2</sub> are formed under the conditions used in the coupled oxidation reaction of the H63V mutant, a solution of hydrazine (0.5 mM) in phosphate buffer, pH 8.5, was continuously bubbled with O<sub>2</sub> at 25 °C, and the concentration of H<sub>2</sub>O<sub>2</sub> was determined after 1 and 2.5 h. These experiments revealed the presence of ~7 and ~14 μM H<sub>2</sub>O<sub>2</sub> after 1 and 2.5 h, respectively, indicating that sufficient H<sub>2</sub>O<sub>2</sub> is accumulated to carry out the coupled oxidation of the mutant. Furthermore, it is likely that more H<sub>2</sub>O<sub>2</sub> is formed but that it is consumed to oxidize hydrazine to HN<sub>3</sub> and NH<sub>3</sub>. It is also important to consider that, in addition to the hydrogen peroxide formed from the oxidation of hydrazine by O<sub>2</sub>, H<sub>2</sub>O<sub>2</sub> might also be formed from a sequence of events in which hydrazine reduces Fe<sup>III</sup>-H63V to the ferrous protein, followed by the binding of O<sub>2</sub> to form the corresponding Fe<sup>II</sup>-O<sub>2</sub> complex. Autoxidation of the oxyferrous complex would produce Fe<sup>III</sup>-H63V and superoxide, and dismutation of the latter would form H<sub>2</sub>O<sub>2</sub>. Alternatively, the Fe<sup>II</sup>-O<sub>2</sub> complex can be reduced by one electron to give the Fe<sup>III</sup>-OOH species, which dissociates to Fe<sup>III</sup>-H63V and H<sub>2</sub>O<sub>2</sub>. The fact that catalase completely inhibits the coupled oxidation of the H63V mutant implies that even if some of the peroxide is formed via the latter mechanism, the coordinated peroxide molecule must dissociate from the protein before it can hydroxylate a *meso* carbon. Consistent with the idea that the Fe<sup>III</sup>-OOH complex of H63V is not conducive to *meso* hydroxylation, when the Fe<sup>III</sup>-H63V mutant is incubated with H<sub>2</sub>O<sub>2</sub> (1, 2, and 4 equiv) in the presence of air, the intensity of the Soret band decreases proportionally to the concentration of H<sub>2</sub>O<sub>2</sub>; however, the spectra collected throughout these experiments clearly show that neither verdoheme nor biliverdin is formed.

These findings clearly demonstrate that although noncoordinated hydrogen peroxide is the oxidant that converts the heme-H63V complex to the corresponding verdoheme complex, this oxidative process cannot be brought about by reacting Fe<sup>III</sup>-H63V with H<sub>2</sub>O<sub>2</sub>, as is the case with heme oxygenase.

- (35) Lagarias, J. C. *Biochim. Biophys. Acta* **1982**, *717*, 12-19.  
 (36) Balch, A. L.; Koerner, R.; Olmstead, M. M. *J. Chem. Soc., Chem. Commun.* **1995**, 873-874.  
 (37) Balch, A. L.; Noll, B. C.; Safari, N. *Inorg. Chem.* **1993**, *32*, 2901-2905.  
 (38) Gilbert, E. C. *J. Am. Chem. Soc.* **1929**, *51*, 2744-2751.

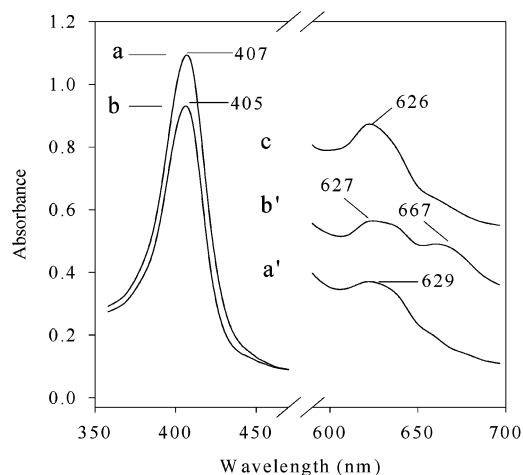


**Figure 4.** (a, a') Electronic absorption spectrum obtained upon treating  $\text{Fe}^{\text{III}}\text{-H63V}$  with 1 equiv of sodium dithionite, followed by the addition of 2 equiv of  $\text{H}_2\text{O}_2$  to the resultant solution of  $\text{Fe}^{\text{II}}\text{-H63V}$ . (b, b') Spectrum obtained when the solution in (a) is exposed to air. The formation of verdoheme is evident from the peak at 667 nm and from a decay in the Soret band. (c) Spectrum obtained when the solution in (b) is bubbled with CO. The peak at 626 nm is characteristic of verdoheme coordinated by a proximal histidine and a distal CO ligand.

An alternative path consistent with the finding that catalase inhibits the coupled oxidation of the heme-H63V complex would entail a reaction between  $\text{Fe}^{\text{II}}\text{-H63V}$  and  $\text{H}_2\text{O}_2$ .

**$\text{H}_2\text{O}_2$  Reacts with  $\text{Fe}^{\text{II}}\text{-H63V}$  To Form Verdoheme via a *meso*-Hydroxyheme Intermediate.** When an anaerobic solution of  $\text{Fe}^{\text{III}}\text{-H63V}$  is treated with 1 equiv of sodium dithionite, the electronic absorption spectrum of the ferric species, which displays a Soret band at 405 nm, is replaced by a spectrum characteristic of  $\text{Fe}^{\text{II}}\text{-H63V}$ , exhibiting a Soret band at 423 nm. Subsequent addition of 2 equiv of an anaerobic solution of  $\text{H}_2\text{O}_2$  to  $\text{Fe}^{\text{II}}\text{-H63V}$  induces time-dependent spectral changes. After approximately 30 min the electronic absorption spectrum does not change any further and displays a Soret band at 407 nm (Figure 4a), and a relatively featureless visible region (Figure 4a'). However, exposing the contents of the cuvette to air results in the formation of verdoheme, as can be seen from the decrease in the intensity of the Soret band (Figure 4b) and the growth of a band at 667 nm (Figure 4b'). Moreover, if the solution is then bubbled with CO, the band at 667 nm decreases in intensity with the concomitant appearance and growth of a band at 626 nm (Figure 4c); the latter is characteristic of verdoheme axially coordinated by a proximal histidine and a distal CO,<sup>12,14,24,39</sup> and therefore provides corroborating evidence that verdoheme is formed upon mixing anaerobic solutions of  $\text{Fe}^{\text{II}}\text{-H63V}$  and  $\text{H}_2\text{O}_2$ , followed by exposure to  $\text{O}_2$ . The relative intensity of the Soret to 667 nm band (curves b and b', respectively, of Figure 4) indicates that the conversion of  $\text{Fe}^{\text{II}}\text{-H63V}$  to verdoheme-H63V is not quantitative; rather, it suggests that less than 30% of the heme is converted to verdoheme. Nevertheless, these results clearly indicate that hydrazine sets the stage for the coupled oxidation to occur by participating in two independent reactions: (a) the reduction of  $\text{Fe}^{\text{III}}\text{-H63V}$  to  $\text{Fe}^{\text{II}}\text{-H63V}$  and (b) the reduction of  $\text{O}_2$  to produce noncoordinated  $\text{H}_2\text{O}_2$ . In turn, noncoordinated  $\text{H}_2\text{O}_2$  and  $\text{Fe}^{\text{II}}\text{-H63V}$  react to produce verdoheme, presumably via a *meso*-hydroxyheme intermediate. In

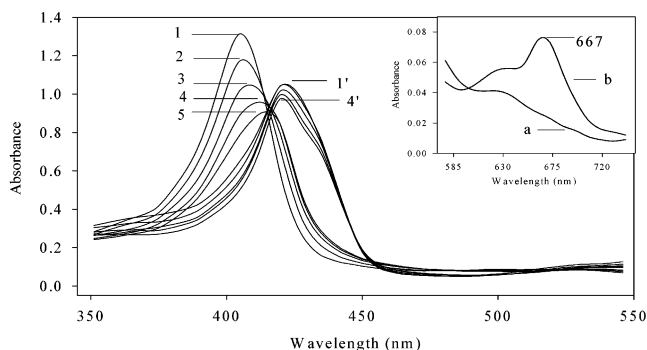


**Figure 5.**  $\text{Fe}^{\text{III}}\text{-H63V}$  (trace 1) was reduced with 1 equiv of sodium dithionite to  $\text{Fe}^{\text{II}}\text{-H63V}$  (trace 1') and then treated with 1 equiv of  $\text{H}_2\text{O}_2$ . The resultant solution (trace 2) was treated with sodium dithionite to produce a solution that gives trace 2', which was again reacted with 1 equiv of  $\text{H}_2\text{O}_2$  to produce a solution that gives trace 3. This cycle was repeated two more times, and spectrum 5 was obtained after the last addition of  $\text{H}_2\text{O}_2$ ; trace a in the inset displays the corresponding visible portion of the spectrum. Exposure of this solution to air results in the formation of verdoheme as is evident from the growth of a peak at 667 nm, trace b in the inset.

fact, as will be shown below, the reaction between  $\text{Fe}^{\text{II}}\text{-H63V}$  and  $\text{H}_2\text{O}_2$  produces *meso*-hydroxyheme, albeit not quantitatively.

When an anaerobic solution of  $\text{Fe}^{\text{III}}\text{-H63V}$ , displaying a Soret band at 405 nm (Figure 5, trace 1), is reduced with 1 equiv of sodium dithionite, the spectrum of the resultant solution displays a Soret band at 423 nm (Figure 5, trace 1'). Subsequent addition of 1 equiv of anaerobic  $\text{H}_2\text{O}_2$  results in a gradual ( $\sim 30$  min) blue shift of the Soret band, which results in a spectrum that exhibits a Soret band at 406 nm (Figure 5, trace 2). If this solution is titrated again with 1 equiv of sodium dithionite, while strict anaerobic conditions are maintained, the resultant solution exhibits a spectrum with a Soret band at 422 nm (Figure 5, trace 2'). When this solution is treated with 1 equiv of an anaerobic solution of  $\text{H}_2\text{O}_2$ , the Soret band shifts to 409 nm (Figure 5, trace 3) over a period of  $\sim 30$  min. This cycle was repeated two more times, resulting in the spectra shown in Figure 5, traces 3' and 4, upon the third reduction with dithionite followed by the addition of 1 equiv of  $\text{H}_2\text{O}_2$ , and traces 4' and 5, upon reduction with dithionite followed by addition of hydrogen peroxide for a fourth time. It is evident that, upon subjecting the H63V mutant to repetitive cycles in which the protein is first reduced with dithionite and then oxidized with  $\text{H}_2\text{O}_2$ , the Soret band, which is initially located at 405 nm, gradually shifts to 417 nm as the number of cycles is increased, whereas the Soret band corresponding to reduced  $\text{Fe}^{\text{II}}\text{-H63V}$  gradually shifts from 423 to 420 nm. These observations suggest that with each cycle the reaction between  $\text{Fe}^{\text{II}}\text{-H63V}$  and  $\text{H}_2\text{O}_2$  leads to the gradual accumulation of a species that is stable under anaerobic conditions. It is possible to hypothesize that this species might be *meso*-hydroxyheme because when air is bubbled through the solution displaying the spectrum shown in Figure 5, trace 5 (the corresponding visible region is shown by trace a in the inset), verdoheme is formed. The formation of verdoheme is apparent from the emergence and growth of a band at 667 nm (trace b in the inset of Figure 5). Additional evidence suggesting that the intermediate accumulated by the repetitive reactions between  $\text{Fe}^{\text{II}}\text{-H63V}$  and  $\text{H}_2\text{O}_2$  is the *meso*-hydroxyheme-H63V complex is described below.

(39) Yoshida, T.; Noguchi, M. *J. Biochem.* **1984**, *96*, 563–570.

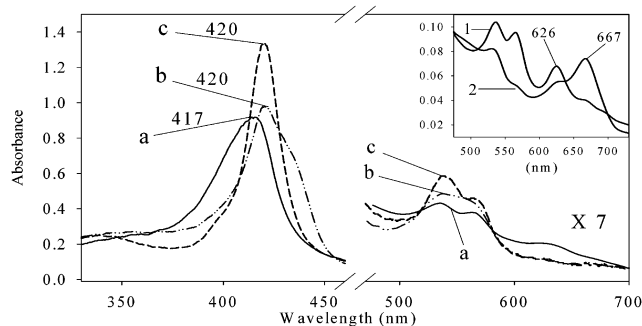


**Figure 6.** (a) Spectrum obtained after a solution of Fe<sup>III</sup>-H63V was treated five consecutive times with 1 equiv of dithionite, followed by 1 equiv of H<sub>2</sub>O<sub>2</sub> (see Figure 5). (b) Spectrum obtained when the solution from (a) is reduced with sodium dithionite, and (c) is the spectrum obtained after the solution from (b) is bubbled with CO. Trace 1 in the inset was obtained after bubbling the solution from (c) with air for 3 min. The peak at 626 nm corresponds to verdoheme coordinated by a proximal His and a distal CO, whereas the peaks at 540 and 567 nm correspond to the  $\beta$  and  $\alpha$  bands of the putative *meso*-hydroxyheme-CO complex. Trace 2 in the inset was obtained after air was bubbled for 15 min. The peak at 667 nm is characteristic of verdoheme.

It is well established that the *meso*-hydroxyheme complexes of heme oxygenase<sup>40,41</sup> and myoglobin<sup>19</sup> react with O<sub>2</sub> to produce the corresponding verdoheme complexes. It has been suggested that ferric *meso*-hydroxyheme is converted to ferric verdoheme by simple exposure to O<sub>2</sub> without the need for a reducing equivalent.<sup>41</sup> An alternative mechanism invoking the need of a reducing equivalent to form ferrous *meso*-hydroxyheme, which subsequently reacts with O<sub>2</sub> to form ferrous verdoheme, has also been proposed.<sup>40,42</sup> More recently it has been suggested that under physiological conditions both reaction pathways might be possible and their relative importance is likely to depend on the concentrations of NADPH, cytochrome P450 reductase, and O<sub>2</sub> in the cell.<sup>43</sup> It is important to point out, however, that there is complete agreement on the fact that in vitro the CO complex of ferrous *meso*-hydroxyheme is converted to the CO complex of ferrous verdoheme when the former is allowed to react with dioxygen.<sup>40-42</sup> In fact, this is a chemical property unique to *meso*-hydroxyheme. Therefore, if the reaction between Fe<sup>II</sup>-H63V and H<sub>2</sub>O<sub>2</sub> does indeed produce *meso*-hydroxyheme, the corresponding CO complex should be converted into the carbomonoxy adduct of the H63V-verdoheme complex upon exposure to air. This hypothesis was tested by performing an experiment in which the putative *meso*-hydroxyheme-H63V complex was first accumulated by means of anaerobically reducing a solution of Fe<sup>III</sup>-H63V with 1 equiv of sodium dithionite, followed by the addition of 1 equiv of an anaerobic solution of hydrogen peroxide, and repeating this cycle four times, as described above. After the last equivalent of an anaerobic solution of H<sub>2</sub>O<sub>2</sub> was added, the resultant solution exhibited a spectrum with a Soret band at 417 nm (Figure 6a). This solution, presumably containing mainly the ferric *meso*-hydroxyheme complex of H63V, was titrated with 1 equiv of sodium dithionite to obtain the corresponding ferrous complex,

which exhibits a Soret band at 420 nm (Figure 6b). When carbon monoxide was bubbled through the resultant solution, while strict anaerobic conditions were still maintained, the electronic absorption spectrum changed from that shown in Figure 6b to the spectrum shown in Figure 6c, which exhibits an intense Soret band at 420 nm and bands at 540 and 567 nm in the visible region. This spectrum is typical of ferrous low-spin hemes axially coordinated by a carbomonoxy ligand and distinct from that exhibited by the CO complex of Fe<sup>II</sup>-H63V, thus indicating that the intermediate accumulated by the repetitive cycles in which Fe<sup>II</sup>-H63V is reacted with H<sub>2</sub>O<sub>2</sub> is capable of forming a carbomonoxy adduct. When the anaerobic solution containing the carbomonoxy adduct of the accumulated intermediate was bubbled with air, the resultant electronic absorption spectra showed the emergence and rapid growth of a band at 626 nm with a concomitant decrease in the intensity of the bands at 540 and 557 nm (trace 1 in the inset of Figure 6). The appearance and growth of a band at 626 nm are diagnostic of the formation of a verdoheme-carbomonoxy complex, axially coordinated by histidine and CO ligands. Upon continued bubbling of air through the solution, the band at 626 nm decreases and disappears, with the simultaneous emergence and growth of a band at 667 nm (trace 2 in the inset of Figure 6); the latter is diagnostic of the presence of the H63V-verdoheme complex. On the basis of these observations, it is possible to conclude that the intermediate species accumulated during the cycles in which Fe<sup>II</sup>-H63V is allowed to react with H<sub>2</sub>O<sub>2</sub> under strict anaerobic conditions is very likely the *meso*-hydroxyheme complex of H63V. Additional evidence demonstrating the formation of *meso*-hydroxyheme was obtained from the EPR spectroscopic experiments described below.

*meso*-Hydroxyheme is known to exist in at least three different resonance forms: a ferric phenolate anion, a ferric keto, and a ferrous keto  $\pi$  neutral radical.<sup>44</sup> The relative contribution of each of these different resonance forms changes upon exposure to CO, which by virtue of coordinating to the iron of *meso*-hydroxyheme stabilizes the ferrous keto  $\pi$  neutral radical species. We took advantage of this property to corroborate the formation of *meso*-hydroxyheme upon reacting Fe<sup>II</sup>-H63V and H<sub>2</sub>O<sub>2</sub>. Thus, Fe<sup>II</sup>-H63V was reacted with 1 equiv of H<sub>2</sub>O<sub>2</sub> under anaerobic conditions, and the resultant solution was frozen in liquid nitrogen to acquire an EPR spectrum at 80 K. The same sample was then thawed out and exposed to CO before a second EPR spectrum was collected. Very weak signals are observed around  $g \approx 6$  and  $g \approx 2$  before exposure to CO (Figure 7A), but exposure to CO results in a  $\sim 40$ -fold increase of the signal around  $g \approx 2$  (Figure 7B). As expected, exposure of the sample to O<sub>2</sub> at room temperature results in the disappearance of the  $g \approx 2$  signal (Figure 7C). The isotropic  $g = 2.006$  signal is typical of an  $S = 1/2$  organic radical, and its appearance upon exposing the solution to CO is clearly indicative of the presence of the ferrous keto  $\pi$  neutral radical structure of *meso*-hydroxyheme.

**Concluding Remarks.** The significance of these findings resides in the fact that the coupled oxidation of hemoproteins has been used as a model to study heme catabolism<sup>15,19,20,22,24,45,46</sup> because it was assumed that it is brought about by coordinated O<sub>2</sub>, which in the presence of a reducing agent, typically

(40) Matera, K. M.; Takahashi, S.; Fujii, H.; Zhou, H.; Ishikawa, K.; Yoshimura, T.; Rousseau, D. L.; Yoshida, T.; Ikeda-Saito, M. *J. Biol. Chem.* **1996**, *271*, 6618-6624.

(41) Liu, Y.; Moënne-Loccoz, P.; Loehr, T. M.; Ortiz de Montellano, P. R. *J. Biol. Chem.* **1997**, *272*, 6909-6917.

(42) Migita, C. T.; Fujii, H.; Matera, K. M.; Takahashi, S.; Zhou, H.; Yoshida, T. *Biochim. Biophys. Acta* **1999**, *1432*, 203-213.

(43) Ortiz de Montellano, P. R.; Wilks, A. *Adv. Inorg. Chem.* **2000**, *51*, 359-407.

(44) Morishima, I.; Fujii, H.; Shiro, Y. *Inorg. Chem.* **1995**, *34*, 1528-1535.

(45) Saito, S.; Itano, H. A. *Proc. Natl. Acad. Sci. U.S.A.* **1982**, *79*, 1393-1397.

(46) Hildebrand, D. P.; Tang, H.-L.; Luo, Y.; Hunter, C. L.; Hunter, M. S.; Brayer, G. D.; Mauk, A. G. *J. Am. Chem. Soc.* **1996**, *118*, 12909-12915.

